

# UC San Diego

## UC San Diego Electronic Theses and Dissertations

### Title

Regulation of the cerebral vascular clock by neural activity

### Permalink

<https://escholarship.org/uc/item/39j408s0>

### Author

Chan, Tamara

### Publication Date

2018

Peer reviewed|Thesis/dissertation

UNIVERSITY OF CALIFORNIA SAN DIEGO

Regulation of the cerebral vascular clock by neural activity

A Thesis submitted in partial satisfaction of the requirements for the degree of  
Master of Science

in

Biology

by

Tamara Cera Chan

Committee in charge:

Richard Daneman, Chair  
Brenda Bloodgood, Co-Chair  
James Cooke

2018



The Thesis of Tamara Cera Chan is approved, and is acceptable in quality and form for publication on microfilm and electronically:

---

---

Co-Chair

---

Chair

University of California San Diego

2018

TABLE OF CONTENTS

Signature Page ..... iii

Table of Contents ..... iv

List of Figures ..... v

List of Tables ..... vi

Acknowledgements ..... vii

Abstract of the Thesis ..... viii

General Introduction ..... 1

Chapter 1: Molecular Plasticity of the Cerebral Vasculature in Response to Neural Activity

    1.1 Introduction ..... 4

    1.2 Materials and Methods ..... 5

    1.3 Results ..... 9

    1.4 Discussion ..... 13

Chapter 2: The Role of the Circadian Clock in the Cerebral Vasculature

    2.1 Introduction ..... 15

    2.2 Materials and Methods ..... 20

    2.3 Results ..... 24

    2.4 Discussion ..... 29

General Discussion ..... 33

References ..... 47

## LIST OF FIGURES

Figure 1. Optimization of DREADDs in glutamatergic neurons .....	37
Figure 2. Global gene expression of endothelial cells after manipulation of neural activity.....	38
Figure 3. Neural activity-dependent genes.....	39
Figure 4. ABC efflux transport function is regulated by neural activity .....	40
Figure 5. Generation of endothelial cell <i>Bmal1</i> conditional knockout .....	41
Figure 6. The endothelial-specific clock regulates time-of-day dependent ABC efflux .....	42
Figure 7. The endothelial-specific clock does not regulate circadian-driven feeding and drinking behaviors .....	43
Figure 8. Endothelial-specific <i>Bmal1</i> knockout does not affect learning and memory.....	44
Figure 9. Endothelial-specific <i>Bmal1</i> knockout displays depression-related behavior, but not anxiety-related behavior .....	45
Figure 10. Brain-endothelial specific <i>Bmal1</i> knockout behavioral trends.....	46

## LIST OF TABLES

Table 1. DAVID Pathway Analysis for 105 genes upregulated after glutamatergic activation and downregulated after glutamatergic activation.....	35
Table 2. DAVID Pathway Analysis for 138 genes upregulated after glutamatergic silencing and downregulated after glutamatergic activation.....	36

## ACKNOWLEDGEMENTS

I would first like to thank my committee chair, Richard Daneman for allowing me to be a part of such a wonderful and wacky lab. I have grown so much as a scientist-in-training, and I thank him for providing me the opportunity to do so. His guidance and expertise have been integral in the trajectory of this project and it would not have gotten this far without his support.

I express my deepest thanks to my mentor, Robert Pulido, who has been a constant teacher and role model from the day I picked up my first pipette. I am very grateful for his extensive contribution to the science presented here, his dedication to the project, and his encouragement throughout the years.

I would like to express gratitude for our collaborators, Stefan Leutgeb and Claire Quirk for taking the time and energy to contribute to this project.

I lastly would like to thank the entire Daneman lab for their contributions, especially Geoffrey Weiner, Mario Malfavon, and Roeben Munji for their expertise, and Aaron Deng for the generous hours he gave.

## ABSTRACT OF THE THESIS

Regulation of the cerebral vascular clock by neural activity

by

Tamara Cera Chan

Master of Science in Biology

University of California San Diego, 2018

Professor Richard Daneman, Chair  
Professor Brenda Bloodgood, Co-Chair

The blood-brain barrier (BBB) is a set of properties belonging to endothelial cells that make up blood vessels in the central nervous system (CNS). The BBB's function is to reduce the transport of nonspecific ions and molecules between the blood and brain and import specific molecules to maintain brain homeostasis. The cerebral vasculature is also known to be tightly coupled to neural activity and dynamically changes blood flow to satisfy the energy demand of active brain regions. Although the cerebral vascular blood flow is tightly coupled to neural activity, the question remains whether BBB properties can dynamically respond to neural activity, as well. Through manipulating glutamatergic neurons in mice, we have shown that neural activity can dynamically regulate both the expression and function of BBB genes in the cerebral vasculature,

namely, ATP- binding cassette (ABC) efflux transporters. Additionally, we found that neural activity dynamically regulates circadian clock-related genes in endothelial cells. This led us to ask the question of what is the functional role of the circadian clock in endothelial cells of the cerebral vasculature? Through knocking out a core clock gene, *Bmal1*, specifically in endothelial cells, we found that the vascular clock regulates ABC efflux transport and animal behavior. We propose the idea that neural activity entrains the vascular-specific circadian clock, which regulates ABC transporter activity in a circadian manner, and deletion of the clock in endothelial cells causes dysregulation of ABC transport, thus disrupting the chemical microenvironment of the brain, resulting in complex behavioral phenotypes.

## GENERAL INTRODUCTION

The blood-brain barrier (BBB) is a set of properties belonging to endothelial cells of the central nervous system (CNS). Together, this set of properties restricts the movement of nonspecific ions and molecules to and from the brain, in addition to importing vital nutrients. By doing so, the BBB maintains homeostatic control of the chemical composition of the brain for proper neuronal function and restricts passage of peripheral immune cells, toxins, and pathogens to protect the brain from neuroinflammation (Zlokovic, 2008). This set of properties consists of tight junctions, efflux transporters, low rates of transcytosis, low expression of leukocyte adhesion molecules, and specific solute transporters. Tight junction proteins highly polarize the endothelial cells, thereby creating a tight seal that restricts the movement of molecules through intercellular space (Anderson & Van Itallie 2009). Efflux transporters, such as P-glycoprotein, contribute to the barrier by exporting lipophilic molecules that would diffuse across endothelial cells, back out into the blood (Cordon-Cardo et al., 1989). In addition, most peripheral endothelial cells use a system of vesicle-mediated transcytosis to transport molecules into the surrounding tissue. However, brain endothelial cells exhibit this characteristic at very low rates (Karnovsky 1968; Hnasko, McFarland, & Ben-Jonathan 2002). Furthermore, peripheral endothelial cells typically express leukocyte adhesion molecules that facilitate transport of immune cells into the tissue (Bevilacqua, 1993; Henninger et al., 1997). However, because entrance of peripheral immune cells into the brain can cause neurotoxicity, brain endothelial cells have low expression of leukocyte adhesion molecules to restrict them from entering the CNS (Engelhardt, 2008). Lastly, in order to transport the nutrients and molecules that are necessary to maintain brain homeostasis and proper neural function, such as glucose, brain endothelial cells highly express solute transporters which have narrow substrate specificities (Simpson, Carruthers, & Vannucci 2007). Collectively, these properties make up the

BBB and tightly regulate exchange of ions and molecules to ensure optimal brain function. These properties are essential for brain homeostasis because breakdown of the BBB and dysfunction of various properties have been shown to contribute to the pathology of various neurological diseases such as multiple sclerosis, epilepsy, stroke, traumatic brain injury, Alzheimer's Disease, and Parkinson's Disease (Zlokovic 2008; Alvarez, Cayrol, & Prat 2011; Lamas, González-Mariscal, & Gutiérrez 2002; Erickson & Banks 2013; Faucheux et al. 1999).

Although the properties of the BBB are expressed by brain endothelial cells, transplantation studies suggest that these properties are not necessarily intrinsic to endothelial cells. In a study where quail embryonic neural tissue was grafted onto mesoderm tissue and was vascularized by mesoderm vessels, the vessels adopted BBB characteristics. On the other hand, when embryonic mesoderm tissue was vascularized by neural vessels, those vessels were devoid of BBB properties (Stewart & Wiley 1981). This suggests that BBB properties are induced by the microenvironment of the neural tissue. In fact, there are two cell types that are closely associated with the vasculature that are known to regulate BBB properties. Pericytes are present during angiogenesis and at the onset of barrier properties, and they are required for BBB formation. On the other hand, astrocytes are proposed to have a critical role in maintaining the BBB throughout adulthood. Their endfeet ensheath endothelial cells and can release many chemical agents that regulate BBB integrity (Igarashi et al. 1999; Abbott, Rönnbäck, & Hansson 2006). Specifically, astrocytes have been shown to induce BBB properties when co-cultured with endothelial cells *in vitro* (Abbott, Rönnbäck, & Hansson 2006).

Although we know that pericytes are essential for formation of the BBB and astrocytes play a role in maintaining its integrity through adulthood, the BBB has largely been studied in a static context. However, the brain is a very dynamic organ with constant fluctuations in neural

activity. Therefore, this thesis will discuss our findings of the dynamic regulation of the BBB by changes in neural activity. Then we will discuss a particular set of genes that was shown to be significantly regulated by neural activity, the circadian clock, and its role in the cerebral vasculature.

## CHAPTER 1: Molecular Plasticity of the Cerebral Vasculature in Response to Neural Activity

### 1.1 Introduction

The brain is a highly energy demanding organ that relies on a constant supply of blood flow to very active areas of the brain. It has been shown that blood vessels of the CNS dilate to increase local blood flow in response to neural activity in order to provide energy and nutrients for this process (Newman, 2013). This relationship between neurons and the cerebral vasculature is called neurovascular coupling. Neurovascular coupling involves communication between neurons and blood vessels through extracellular potassium and glutamate-evoked release of nitric oxide from neurons, acting on smooth muscle to cause vasodilation, and hence, increase regional blood flow (Fergus & Lee, 1997; Howarth, 2014; Longden et al., 2017). Although we know that neurons dynamically communicate with the cerebral vasculature in the biophysical context of blood flow, little is known about molecular changes happening in endothelial cells during this phenomenon. We postulated that neural activity could dynamically regulate cerebral vascular properties on a molecular level, as well.

An experiment performed previously in the lab preliminarily supports our hypothesis that neural activity may have dynamic control over cerebral vascular properties. The experiment asked what changes are occurring at the BBB on the molecular level in response to epileptic seizures, characterized by excess neural activity that causes BBB breakdown. We analyzed the BBB transcriptome in an epilepsy mouse model at different time points: an acute time point 2 hours after injection of kainic acid (point of peak epileptic symptoms), and a sub-acute time point 48 hours after injection (point of ceased neural activity but extensive BBB breakdown). We found that many unique BBB genes were upregulated and downregulated only at the acute time point,

but returned to baseline levels at the sub-acute time point. Many of these changes in gene expression that we observed at the acute time point were unique to the seizure model in comparison to other disease models that have BBB breakdown. Since these unique changes occurred at the acute time point, when the biggest change in neural activity was occurring, and did not persist for the sub-acute time point, when BBB breakdown was taking place, this led us to hypothesize that many of the seizure-related molecular changes in the cerebral vasculature that occurred could be regulated by neural activity, rather than pathology.

To investigate how the cerebral vasculature is dynamically regulated by changes in neural activity, we utilized the pharmacogenetic tool Designer Receptors Exclusively Activated by Designer Drugs (DREADDs) to manipulate neural activity specifically in glutamatergic neurons (glutamate is the main excitatory neurotransmitter of the brain). Then, we isolated the brain endothelial cell RNA and analyzed the brain endothelial cell transcriptome to observe BBB property changes in response to increases or decreases in neural activity.

## 1.2 Materials and Methods

### *Transgenic mice and treatments*

Wild-type mice with c57BL/6 background were obtained from Envigo. To create transgenic mice in which we can control glutamatergic activity, we crossed *CamKIIa-tTA* mice (Jackson Laboratory 007004) to *TRE-GqDREADDs* (Jackson Laboratory 014093) to increase glutamatergic activity and *TRE-GiDREADDs* (Jackson Laboratory 024114) to silence glutamatergic activity. All experiments were performed in adult mice 3-4 months of age.

### *Immunohistochemistry*

Mice were anaesthetized with a ketamine (100 mg kg<sup>-1</sup>)/xylazine (20 mg kg<sup>-1</sup>) and then perfused with PBS followed by 4% paraformaldehyde for 7 minutes. Dissected brains were stored in 30% sucrose in PBS overnight at 4°C. Brains were frozen down in 1:2 30% sucrose:OCT mixture. 40 micrometer floating tissue cryosections were prepared. Floating sections were incubated in a blocking solution of 5% goat serum and 0.1% Tween-20 (Fisher Scientific BP337-100) in PBS for 45 minutes at room temperature, followed by incubation in primary antibody solution of Rabbit anti HA at a dilution of 1/250 (Cell Signaling Technology, 3724) overnight at 4°C. Appropriate secondary antibodies, conjugated to Alexa fluorophores, were incubated for 1.5 hours at room temperature before mounting with DAPI Fluoromount-G® (SouthernBiotech, 0100-20). All pictures were taken and analyzed with AxioVision.

### *Multi-electrode Array Recordings*

DREADDs mice underwent stereotaxic surgeries to implant multielectrode arrays in the cortex and hippocampus as described previously<sup>24</sup>. Mice recovered for 3 weeks. 15 minutes of recording established a baseline and then a given dose of Clozapine-N-Oxide (CNO) (Enzo, BML-NS105-0005) was administered through intraperitoneal injection. The dose used for Gq-DREADDs mice was 0.5 mg/kg and the dose used to Gi-DREADDs mice was 1 mg/kg. The electrodes recorded for 3 hours post-injection. Neuralynx software was used to record signaling unit firing, locomotor behavior, and local field potential.

### *Fluorescence Activated Cell Sorting (FACS)*

Mice were collected in pairs of one experimental and one littermate control for each manipulation (glutamatergic activating and glutamatergic silencing). Each mouse was injected with the verified dose of CNO (0.5mg/kg for glutamatergic activating, 1mg/kg for glutamatergic silencing, 1mg/kg for astrocyte activating). Behavior was monitored closely for 3 hours post-injection before animals were euthanized with a small rodent guillotine. If seizures were observed via stalling or convulsive behavior in the glutamatergic activating mice, the mice were euthanized and the experiment was aborted. The brains were dissected out, meninges were removed, and the cortex and hippocampus were harvested. The tissue was then diced with a #10 scalpel and dissociated in Papain (Worthington Biochemical Corporation) for 90 minutes on a 33°C heat block while feeding 5% CO<sub>2</sub>/95% O<sub>2</sub> gas. The tissue was triturated and then a second enzymatic dissociation was performed in 1.0mg/ml Collagenase Type 2 (Worthington Biochemical Corporation), 0.4mg/ml Neutral Protease (Worthington Biochemical Corporation) solution for 30 minutes on a 33°C heat block while feeding 5% CO<sub>2</sub>/95% O<sub>2</sub>. Myelin was removed as recommended by MACS Miltenyi Biotec protocol. The remaining cell suspension was blocked with Rat IgG 1:100 (Sigma Aldrich, I8015) and stained with Alexa647 rat anti CD31 1/100 dilution (Molecular Probes, A14716), FITC anti CD45 1/100 dilution (eBioscience, 11-045185), FITC rat anti CD13 (BD Pharmingen, 558744), FITC anti CD11b (eBioscience, 11-0112-81), 488 rabbit anti NG2 (Bioss, bs-11192R-A488), and DAPI. CD31 positive cells were purified and sorted into TRIzol reagent (Ambion, 10296010) at the Flow Core at the VA Hospital in San Diego. FACS prep was performed 4 times to give 4 pairs of mice in each manipulation condition.

### *RNA Sequencing*

For glutamatergic activating and glutamatergic silencing mice, RNA was purified with the Qiagen RNA Isolation Microkit. After purification, the RNA was run on a tape station bioanalyzer at the UCSD Genomics Core to assess purity and concentration. A cDNA library was prepared TruSeq RNA Library Prep Kit v2 (Illumina). Samples were then sequenced on an Illumina HiSeq4000, 150 based, paired ends. Sequence reads for all samples were mapped to Ensembl mm9 v67 mouse whole genome using Tophat v 2.0.11 and Bowtie 2 v 2.2.1 with parameters no-coverage-search -m 2 -a 5 -p 7. Alignment files were sorted using SAMtools v.0.1.19. Count tables were generated using HTSeq-0.6.1. Differential expression of genes between control and treated samples, log 2-fold changes between control and treated samples, and statistical analysis including p values and FDR was performed using DESeq2 and Excel.

### *Rhodamine123 Permeability*

Mice were collected in pairs of one experimental and one littermate control for each manipulation (glutamatergic activating and glutamatergic silencing). Each mouse was injected with the verified dose of CNO (0.5mg/kg for glutamatergic activating, 1mg/kg for glutamatergic silencing). Two hours after CNO injection, each mouse was injected with rhodamine123 (Sigma Aldrich, 83702) at a dose of 25mg/kg. Two hours after rhodamine123 injection, mice were anaesthetized with a ketamine (100 mg kg<sup>-1</sup>)/xylazine (20 mg kg<sup>-1</sup>) and blood was collected via cardiac punch. The mice were then perfused with PBS and the brains were dissected out, meninges were removed, and the cortex and hippocampus were harvested. The blood was centrifuged at 2000g for 15 minutes to obtain plasma. The brains were homogenized in cold PBS (volume adjusted to the weight of the brain). For both the homogenized brains and the plasma, butanol

extraction was performed and rhodamine fluorescence was quantified via spectrofluorimetry (Tecan Infinite 200 Pro) with excitation wavelength of 505nm and emission wavelength of 560nm.

### 1.3 Results

#### *Glutamatergic DREADDs localization*

To manipulate neural activity, we utilized designer receptors exclusively activated by designer drugs (DREADDs). They are engineered G-protein coupled receptors (GPCRs) that are activated by an inert, exogenous drug called clozapine-N-oxide (CNO), and is an established tool to manipulate the activity of neurons *in vivo* (Alexander et al., 2009). DREADDs that are coupled to Gq proteins will induce neuronal activation, and those coupled to Gi proteins will induce neuronal silencing. To express Gq- and Gi-DREADDs in glutamatergic projection neurons, *CamKIIa-tTA* mice were crossed to *TRE-GqDREADDs* and *TRE-GiDREADDs* (Figure 1A), which allowed us to use the Tet Off system to express the DREADDs under the CamKIIa promoter that is predominantly expressed in glutamatergic pyramidal neurons. This pharmacogenetic tool allowed us to manipulate neural activity both spatially and temporally.

The DREADDs transgene was designed to include a human influenza hemagglutinin (HA) tag on the N-terminus. Therefore, we used immunohistochemistry with an antibody against HA to visualize where the DREADDs were localized in the brain. We found that they were predominantly localized to the cortex and hippocampus, consistent with the localization of glutamatergic pyramidal neurons (Figure 1B).

### *Optimization of CNO dosage for neural activity manipulation*

After visualizing the localization of the DREADDs, we optimized the tool by finding the ideal dosage of CNO needed to illicit the largest change in neural activity and characterizing the pharmacodynamic profiles *in vivo* using multi electrode array recordings. Using stereotaxic surgery, we implanted electrodes into the cortex and hippocampus to record local field potential (LFP).

We performed multiple recordings in mice expressing DREADDs in glutamatergic neurons and their respective littermate controls. As expected, control mice that do not express the DREADDs had no change in LFP power in response to a dose of 1.0 mg/kg CNO (Figure 1C). For mice that express the Gq-DREADDs in glutamatergic neurons, we determined that a dose of 0.5 mg/kg CNO was the highest possible dose that did not induce seizures in the animals, and thus served as the dose we used for all experiments. An increase in gamma LFP power was observed at approximately 75 minutes after 0.5 mg/kg CNO injection and persisted for the entire duration of the three hour recording session (Figure 1D). Mice that expressed the Gi-DREADDs in glutamatergic neurons exhibited a robust attenuation of LFP power in response to 1.0 mg/kg of CNO (Figure 1E). Therefore, we determined the ideal dosages to cause robust activation and silencing of glutamatergic DREADDs to be 0.5 mg/kg and 1 mg/kg, respectively. These data showed that we could successfully manipulate neural activity by expressing DREADDs in glutamatergic neurons.

### *Cerebral vascular genes are regulated by neural activity*

Using these optimal dosages of CNO, we injected DREADDs mice and a littermate controls, purified brain endothelial cells by fluorescence activated cell sorting (FACS), and

performed RNA sequencing to measure the brain endothelial cells' transcriptomic response to these perturbations in neural activity (Figure 2A).

After activation of neural activity through glutamatergic DREADDs, RNA sequencing analysis revealed 624 significantly upregulated genes and 748 significantly downregulated genes (Figure 2B). After silencing glutamatergic activity, there were 718 significantly upregulated genes and 603 significantly downregulated genes (Figure 2D). When the two datasets were compared, we found 243 genes total whose expression changed in opposite directions after activation versus silencing of neural activity (Figure 3A). This suggests that the expression levels of these 243 brain endothelial cell genes are regulated by the amount of neural activity in the brain.

We performed pathway analysis using the DAVID Bioinformatics Database to get a global view of what these 243 neural activity-regulated genes are involved with. Within those 243 genes, 105 of them were significantly upregulated after glutamatergic activation and significantly downregulated after glutamatergic silencing. Pathway analysis revealed an enrichment in genes mostly involved in adherens junctions, which stabilize cell-to-cell contact and regulate the actin cytoskeleton, and focal adhesions, which link the endothelial cells to the extracellular matrix and are important for sensing blood flow (Table 1). Both of these pathways were likely upregulated in glutamatergic activation and downregulated in silencing as a response to shear stress from local blood flow changes.

On the other hand, there were 138 genes that were significantly upregulated after glutamatergic silencing and significantly downregulated after glutamatergic activation. Pathway analysis revealed two of the top five enriched gene groups were ABC (ATP-binding cassette) transporters and bZip (basic-leucine zipper domain) transcription factors (Table 2). Neural activity-dependent changes in ABC transporters, which are the major class of efflux transporters

and a hallmark BBB property, suggests that the BBB is transiently altering permeability in response to neural activity specifically through ABC efflux transporters. They were upregulated in response to glutamatergic silencing and downregulated in response to glutamatergic activation. The four specific ABC transporters that were upregulated during glutamatergic silencing and downregulated during glutamatergic activation were *Abcb1a* (*P-glycoprotein*), *Abcc4* (*MRP4*), *Abca3* and *Abcd4* (Figure 3B).

The second gene group of interest that was regulated by neural activity was the bZip transcription factors, also called the PAR (proline and acidic amino acid-rich) bZip transcription factors: *Tef*, *Hlf*, and *Dbp* (Figure 3C). These are circadian clock-controlled genes that regulate the transcription of many downstream targets. Their upregulation in glutamatergic silencing and downregulation in glutamatergic activation suggests that circadian clock within the cerebral vasculature changes in response to perturbations of neural activity. This will be further discussed in Chapter 2.

#### *ABC transporter function is regulated by neural activity*

To follow up on the dynamic regulation of ABC transporter expression by neural activity, we performed a rhodamine permeability assay to investigate ABC transporter function in response to glutamatergic activation and silencing. Rhodamine123 (RH123), a lipophilic fluorescent dye, is an exogenous substrate of P-gp, the major ABC transporter in the mammalian BBB. We injected the DREADDs mice and littermate controls with CNO, then injected RH123, then collected the brains and blood two hours later. If *P-gp* expression is upregulated with neuronal silencing and downregulated with neuronal activation, we expect to see correlative changes in the amount of RH123 that enters the brain tissue from the blood.

After glutamatergic activation, we saw an increase in the amount of RH123 fluorescence in the brain (normalized to the blood) relative to littermate controls (Figure 4). A greater amount of RH123 in the brain indicated that P-gp, whose normal function is to export RH123 and other substrates from the brain tissue back out into the blood, was functioning less efficiently compared to its littermate controls. After glutamatergic silencing, we saw a decrease in the amount of RH123 fluorescence in the brain (normalized to the blood) relative to littermate controls. This indicated that P-gp function was higher in the neuronal silencing condition compared to its littermate controls. This suggests that dynamic increases or decreases in neural activity can alter the BBB on both the molecular and functional level with respect to ABC transporters.

## 1.4 Discussion

Through transcriptomic analysis of brain endothelial cells in response to perturbations in neural activity, we showed an array of endothelial genes that were directly dependent on the amount of glutamatergic activity. They were significantly changed in opposite directions between activation and silencing of glutamatergic activity. Many of these neural activity-dependent genes were involved in BBB properties, most notably several genes in the class of efflux transport proteins called ABC transporters, which were upregulated in glutamatergic silencing and downregulated in glutamatergic activation. The role of efflux transporters at the BBB is to pump small lipophilic molecules that may have diffused across the luminal side of endothelial cells back out into the blood. Therefore, their upregulation in neuronal silencing suggests that the BBB is responding to the decreased neural activity by upregulating expression of ABC transporters in order to decrease permeability. Their downregulation in response to neuronal activation suggests that the BBB is responding to the increased neural activity by downregulating expression of ABC

transporters in order to increase permeability. Furthermore, we confirmed that the expression changes are causing a functional change at the BBB using a rhodamine permeability assay. Increases in neural activity caused a transient P-gp-mediated increase in BBB permeability to RH123, while decreases in neural activity caused a transient P-gp-mediated decrease in BBB permeability to RH123. This is consistent with the RNAseq data that showed neuronal activation led to downregulation of P-gp and neuronal silencing led to upregulation of P-gp.

The identification that BBB permeability to RH123 is regulated by neural activity raises the likelihood that permeability to the vast number of other P-gp substrates are regulated by neural activity as well. P-gp is most well known to efflux xenobiotic drugs, hence the difficulty in getting drugs into the brain. Our results suggest that P-gp function may be changed even transiently through increases or decreases in neural activity, where greater activity could lead to enhanced drug uptake into the brain. Furthermore, amyloid beta, the peptide that accumulates in the brains of Alzheimer's patients, has been proposed to be a substrate of P-gp. Our results suggest that decreases in neural activity could lead to enhanced clearance of amyloid beta, and therefore slow the progression of the disease. Overall, RNA expression and functional changes in P-gp suggest that the cerebral vasculature is dynamically responding to transient changes in neural activity by regulating the chemical microenvironment of the brain, which can have major implications for drug delivery and treatment of neurological diseases.

## CHAPTER 2: The Role of the Circadian Clock in the Cerebral Vasculature

### 2.1 Introduction

As discussed in Chapter 1, we showed that neural activity dynamically controls expression of many endothelial cell genes, including the PAR bZip transcription factors *Tef*, *Hlf*, and *Dbp*. These three genes have been shown to have strong oscillatory nature in tissues, such as the SCN and liver, and *Dbp* has been shown to be directly regulated by the core circadian clock machinery (Rgen, Ripperger, Shearman, Reppert, & Schibler, 2000). Interestingly, mice deficient in all three PAR bZip transcription factors in all cells in the body are prone to lethal epileptic seizures, indicating a role for these factors in neuronal function (Gachon et al., 2004). It has also been shown that the PAR bZip transcription factors regulate downstream target genes that are involved in sensing, metabolizing, and transporting xenobiotic substances in the liver, including some ABC transporters (Gachon, Olela, Schaad, Descombes, & Schibler, 2006). Our findings, suggesting that these clock-related genes in endothelial cells of the brain are directly regulated by neural activity, and the literature, showing their global involvement in brain function and xenobiotic transport, led us to question whether the circadian clock in the cerebral vasculature has a role in regulating the BBB and neuronal function.

The circadian clock is an endogenous biological rhythm that governs the oscillation of a variety of physiological processes, such as sleep, renal activity, heart rate, gastrointestinal tract motility, immune response, and metabolism (Richards & Gumz 2012). The clock is essential for entraining circadian rhythmicity of these processes. Cells have an endogenously oscillating transcriptional feedback loop consisting of a positive and negative loop. Although endogenously oscillating, this transcriptional loop can be entrained by extrinsic cues in the environment, such as light. The key drivers of the positive feedback loop are transcription factors CLOCK and BMAL1.

The CLOCK/BMAL1 heterodimer binds to E box enhancers to activate transcription of *period* and *cryptochrome* genes. The resulting mPER and mCRY proteins act as negative regulators by inhibiting the transcription of *Clock* and *Bmal1*. As mPER and mCRY proteins get degraded over time, inhibition of *Clock* and *Bmal1* is released, thus allowing CLOCK and BMAL1 levels to rise again (Ripperger & Schibler 2001; Reppert & Weaver 2001). These oscillations in clock proteins create an intrinsic rhythm in cells that express these genes and therefore, can regulate physiological activities associated with those genes.

Circadian rhythmicity is most well characterized in the neurons of the suprachiasmatic nucleus (SCN). The SCN is considered the master clock of the body that highly expresses the oscillatory clock genes and exhibits autonomous oscillation in neuronal firing rate over a 24 hour period (Welsh, Logothetis, Meister, & Reppert, 1995). Although these cells can operate a circadian rhythm autonomously through the underlying molecular machinery, they are also entrained by light. Light from the environment is received by melanopsin-expressing retinal ganglion cells in the eye causing increase in membrane potential; these retinal ganglion cells then directly innervate the neurons of the SCN via the retinohypothalamic tract (Reppert & Weaver 2002). The SCN's entrainment by external light allows our body to maintain a synchronous rhythm with the environment and also adapt to environmental changes.

Although the circadian transcriptional machinery has been largely studied in the SCN, more recent findings suggest that the same machinery is highly expressed in a wide variety of non-neuronal cell types and peripheral tissues, including the vasculature. In studies investigating the clock's role in regulating vascular tone, or the diameter of blood vessels as a result of smooth muscle constriction and relaxation, *Bmal1* has been shown to regulate diurnal properties of mean arterial pressure. Arterial pressure increases during the active phase and decreases during the

inactive phase. When *Bmal1* is knocked out globally, this diurnal regulation of mean arterial pressure is eliminated (Curtis et al., 2007). Subsequently, it was shown that the abolishment of diurnal variation in blood pressure via global *Bmal1* knockout leads to hypertension via the uncoupling of endothelial nitric oxide synthase. (Anea et al., 2012; Jacob Richards, Diaz, & Gumz, 2014; Sandoo, van Zanten, Metsios, Carroll, & Kitas, 2010). Furthermore, Durgan et al. (2017) demonstrated the functional importance of a circadian clock in brain vasculature *ex vivo*. They isolated cerebral arteries and measured *Bmal1* and other clock component mRNA at different times of day and found peak levels *Bmal1* during the sleep phase and conversely, peak levels of *per1* and *per2* during the active phase. Correspondingly, isolated cerebral arteries also showed differential sensitivity to vasodilator ATP in a diurnal fashion. To investigate the clock's influence on endothelial function, they induced obstructive sleep apnea and found that peak expression level of some clock components declined. With this disruption of the circadian clock in endothelial cells, the previously shown diurnal rhythm of ATP-sensitive vasodilation was abolished (Durgan, Crossland, & Bryan 2017). Altogether, the cerebral vasculature has been shown to have a circadian clock that causes differential day and night vasodilating ability in response to ATP, which is likely necessary to meet differential energy demands of the brain during the active and inactive phases.

Not only has the clock been implicated in regulating vascular tone, but also in regulating BBB permeability and neuroinflammation. A previous study revealed that brain-specific germline *Bmal1* knockout mice exhibit severe age-dependent astrogliosis, which is often a response to neuroinflammation (Musiek et al. 2013). Subsequently, Nakazato et al. (2017) determined that the same this same brain-specific germline *Bmal1* knockout led to BBB hyperpermeability via loss of pericyte coverage on endothelial cells, thereby providing a link between BBB leakage of blood-derived factors into the brain tissue and subsequent astrogliosis (Nakazato et al. 2017). The results

indicate that *Bmall* expression in the brain is crucial to upholding BBB integrity and protecting the brain from neuroinflammation via regulating pericyte coverage on endothelial cells. However, because this was discovered using a germline knockout specifically in neurons and glia, it does not address the potential BBB role for the circadian clock residing within endothelial cells. Furthermore, in the *Drosophila* brain, xenobiotic efflux is regulated in a circadian manner by a molecular clock in the BBB (Zhang et al. 2018). Considering that the *Drosophila* BBB is composed of glial cells, we cannot draw a direct analogy to the mammalian BBB. However, it does warrant an endothelial cell-specific investigation into the circadian clock's potential regulation of ABC efflux transport in the mammalian BBB.

Additionally, we have shown that neural activity dynamically controls expression of many endothelial cell genes. Specifically, we saw decreased PAR bZip transcription factor expression after inducing neural activity, and increased expression after silencing neural activity. Since we saw dynamic regulation of clock genes by manipulating neural activity, it led us to ask whether manipulating clock gene expression could reciprocally regulate brain function. Therefore, we asked the question of how abolishing *Bmall* in endothelial cells could have an effect on neural activity, and hence, behavior.

The research aim is to further examine the role of the circadian clock in endothelial cells of the brain vasculature. As previously noted, the current literature characterizes the role of the clock in three main aspects of the vasculature. Firstly, it has been implicated in the regulation of vascular tone. However, the studies performed on global *Bmall* knockout mice only examined peripheral blood pressure changes, and the studies performed in cerebral arteries were only observational and performed *ex vivo*, therefore they carry limitations to our understanding of the clock's endogenous function in the brain vasculature. Secondly, the clock has been implicated in

maintaining BBB integrity via regulating pericyte coverage on endothelial cells. This was performed using a *Nestin-Cre* driven *Bmal1* knockout mouse, which targets ablation in neuronal and glial cell precursors. This leads to the question of whether the BBB will also be compromised if *Bmal1* was knocked out in the actual cell type that possesses BBB properties, the endothelial cells. Lastly, our studies using glutamatergic DREADDs have shown that clock-controlled PAR bZip transcription factors are regulated by neural activity. Their functions have largely been studied in the SCN and the liver, where they have been shown to affect neuronal function and xenobiotic efflux, however this was only studied using global triple knockouts of *Tef*, *Hlf*, and *Dbp*. We asked the question of how disrupting these clock-controlled genes via knocking out the clock entirely in endothelial cells can affect brain vasculature and whether this cell-specific disruption can lead to altered neuronal function and xenobiotic efflux.

To address some of the limitations and unanswered questions surrounding the role of *Bmal1* in the cerebral vasculature, we created two inducible genetic *in vivo* knockout models, namely *Slco1c1-CreERT2* conditional knockout and a *VECadherin-CreERT2* conditional knockout, to ablate *Bmal1* in brain-specific and whole-body endothelium postnatally once the vasculature is fully formed. With these models, we investigated *Bmal1*'s role in regulating ABC efflux transport at the BBB and whether these changes in the cerebral vascular clock can affect behavioral phenotypes. We hope to further elucidate the functional role of clock gene *Bmal1* in endothelial cells of the cerebral vasculature.

## 2.2 Materials and Methods

### *Transgenic mice and treatments*

Wild-type mice with c57BL/6 background were obtained from Envigo. *VE-Cadherin-CreERT2* (MGI:3848982) mice were gifted to us from Ralf Adams and *Slco1c1-CreERT2* (MGI:5301361) mice were gifted to us from Markus Schwaninger. To knockout *Bmal1* in whole body endothelium, we crossed *VE-Cadherin-CreERT2* mice to mice with a loxP-flanked basic helix-loop-helix (bHLH) domain of *Bmal1* (Jackson Laboratory 007668) to create *Bmal1<sup>fl/fl</sup>; VECad-CreERT2* mice and genetic controls (*Bmal1<sup>fl/fl</sup>*). To confirm Cre-recombination, *Bmal1<sup>fl/fl</sup>; VECad-CreERT2* mice were then crossed to a *Rosa-loxstoplox-tdTomato* reporter mouse (Jackson Laboratory 007908) to analyze by immunohistochemistry. To knockout *Bmal1* in brain endothelium, we crossed *Slco1c1-CreERT2* mice to mice with a floxed *Bmal1* to create *Bmal1<sup>fl/fl</sup>; Slco1c1-CreERT2* mice and genetic controls (*Bmal1<sup>fl/fl</sup>*). All mice were injected at five weeks of age with three 100 $\mu$ l doses of 20mg/ml tamoxifen (Sigma, T5648) dissolved in corn oil (Sigma-Aldrich, C8267). All experiments were performed between 6 to 8 weeks after tamoxifen treatment.

### *Fluorescence Activated Cell Sorting (FACS)*

Mice were collected in pairs of one experimental (*Bmal1<sup>fl/fl</sup>; VECad-CreERT2*) and one littermate control (*Bmal1<sup>fl/fl</sup>*). Mice were euthanized under CO<sub>2</sub>, brains were dissected out, meninges were removed, and the cortex and hippocampus were harvested. The tissue was then diced with a #10 scalpel and dissociated in Papain (Worthington Biochemical Corporation) for 90 minutes on a 33°C heat block while feeding 5% CO<sub>2</sub>/95% O<sub>2</sub> gas. The tissue was triturated and then a second enzymatic dissociation was performed in 1.0mg/ml Collagenase Type 2

(Worthington Biochemical Corporation), 0.4mg/ml Neutral Protease (Worthington Biochemical Corporation) solution for 30 minutes on a 33°C heat block while feeding 5% CO<sub>2</sub>/95% O<sub>2</sub>. Myelin was removed as recommended by MACS Miltenyi Biotec protocol. The remaining cell suspension was blocked with Rat IgG 1:100 (Sigma Aldrich, I8015) and stained with Alexa647 rat anti CD31 1/100 dilution (Molecular Probes, A14716), FITC anti CD45 1/100 dilution (eBioscience, 11-045185), FITC rat anti CD13 (BD Pharmingen, 558744), FITC anti CD11b (eBioscience, 11-0112-81), and DAPI. CD31 positive cells were purified and sorted into TRIzol reagent (Ambion, 10296010) at the Flow Core at the VA Hospital in San Diego.

### *PCR*

Multiplex PCR was performed on endothelial and nonendothelial cell populations isolated by FACS in both *Bmal1<sup>fl/fl</sup>*, *VECad-CreERT2* and *Bmal1<sup>fl/fl</sup>* mice. Each group of cells was lysed with Proteinase K (Viagen, 501-PK) in DirectPCR Lysis Reagent (Viagen, 102-T), then incubated rotating overnight at 55°C. Lysates were incubated at 85°C for 45 minutes to inhibit Proteinase K. Genotyping was performing using primers L1, ACTGGAAGTAACTTTATCAAAGT; L2, CTGACCAACTT GCTAACAATTA (reverse primer); and R4, CTCCTAACTTGGTTTTT GTCTGT (Storch et al., 2007).

### *Immunohistochemistry*

Mice were anaesthetized with a ketamine (100 mg kg<sup>-1</sup>)/xylazine (20 mg kg<sup>-1</sup>) and then perfused with PBS followed by 4% paraformaldehyde for 5 minutes. Dissected brains were stored in 30% sucrose in PBS overnight at 4°C. Brains were frozen down in 2:1 30% sucrose:OCT mixture. 10 micrometer tissue cryosections were prepared. Sections were incubated in a blocking

solution of 5% goat serum and 0.1% Triton X-100 in PBS for 45 minutes at room temperature, followed by incubation in primary antibody solution of rat anti mouse CD31 at a dilution of 1/250 (BD Pharmingen, 553370) overnight at 4°C. Secondary antibody goat anti rat conjugated to Alexa 488 (Life Technologies, A11006) was incubated for 1.5 hours at room temperature before mounting with DAPI Fluoromount-G® (SouthernBiotech, 0100-20). All pictures were taken and analyzed with AxioVision.

#### *Rhodamine permeability*

RH123 (Sigma Aldrich, 83702) was injected 1.5 hours prior to each time point at a dose of 25mg/kg. Two hours after RH123 injection, mice were anaesthetized with a ketamine (100 mg kg<sup>-1</sup>)/xylazine (20 mg kg<sup>-1</sup>). Blood was collected via cardiac punch and the mice were then perfused with PBS. The brains were dissected out, meninges were removed, and the cortex and hippocampus were harvested. The blood was centrifuged at 2000g for 15 minutes to obtain plasma. The brains were homogenized in cold PBS (volume adjusted to the weight of the brain). For both the homogenized brains and the plasma, butanol extraction was performed as described previously with weight/volume adjusted (Banes et al. 1986). Rhodamine fluorescence was quantified via spectrofluorimetry (Tecan Infinite 200 Pro) with excitation wavelength of 505nm and emission wavelength of 560nm.

#### *Food and water measurements*

Mice were single-housed with *ad libitum* access to food and water in a standard 12-hour LD cycle. Food intake was measured by weight of the food in grams and water intake was

measured as the displacement of water in a cylindrical tube fixed with a drinking spout. Measurements were taken at ZT 0 and ZT 12 every day over a period of four days.

#### *Novel object recognition (NOR) test*

Mice were acclimated to the testing room with for 30 minutes prior to experiment. All NOR tests were performed with minimal ambient lighting to minimize anxiety-inducing stressors. The mice were allowed one 5 minute habituation period inside the testing box, define as Trial 1. They were allowed three consecutive 5 minute habituation periods inside the box with two identical objects, defined as Trials 2-4. After Trial 4, one object was switched for a novel object of different shape, color, and material. Investigative behavior towards an object was defined as head oriented toward the object within 1.0 cm, sniffing of the object, or deliberate contact with the object (deliberate contact with the object but head orientated away was not scored as investigative). Videos were scored manually by an experimenter blind to genotype. Discrimination index (DI) was calculated as time spent exploring novel object subtracted by time spent exploring the old object, divided by the total exploration time.

#### *Open field test*

Mice were acclimated to the testing room with for 30 minutes prior to experiment. The testing box contained an inner concentric square drawn on the floor that delineated inside versus outside. Mice were placed in the testing box for a single 5 minute period. Time inside was defined as more than half of the body inside the inner square. Half of the body inside the inner square was only considered “inside” if the head was orientated toward the center of the square. Videos were scored manually by an experimenter blind to genotype.

### *Tail suspension test*

Mice were acclimated to the testing room with for 30 minutes prior to experiment. Mice were fitted with a short tube covering the tail to prevent tail-climbing, and then were suspended by the tail with tape such that they cannot touch the ground or nearby surfaces. The mice were suspended for a single 6 minute period in which immobility (as opposed to escape-orientated behavior) was characterized by complete lack of movement, other than movement necessary to breathe. Videos were scored manually by an experimenter blind to genotype.

## 2.3 Results

### *Bmal1 Knockout Confirmation*

To knockout *Bmal1* in all endothelium, we obtained a *VECadherin*-CreERT2 transgenic mouse and crossed it to a loxP-*Bmal1*-loxP transgenic mouse to create our conditional endothelial *Bmal1* knockout model (*Bmal1*<sup>fl/fl</sup>; *VECad*-CreERT2) (Figure 5A). Therefore, upon tamoxifen injection, the activated Cre-recombinase enzyme excises the loxP sites, resulting in genetic deletion of the basic helix-loop-helix (bHLH) domain (exon 8) of *Bmal1*, rendering the protein nonfunctional (Figure 5B). To confirm the knockout as well as its cell specificity, we used six weeks post-tamoxifen *Bmal1*<sup>fl/fl</sup>; *VECad*-CreERT2 mice and littermate controls (*Bmal1*<sup>fl/fl</sup>) mice to isolate both endothelial cell and non-endothelial cell populations from each mouse via FACS. Then we PCR-amplified the conditional allele, as well as the excised allele in each condition. For *Bmal1*<sup>fl/fl</sup> mice, gel electrophoresis indicated that both endothelial cells and non-endothelial cells had the intact conditional allele (as indicated by 0.43 kb band size). For *Bmal1*<sup>fl/fl</sup>; *VECad*-CreERT2 mice, endothelial cells had the excised allele (0.57 kb band) while non-endothelial cells had the

intact conditional allele, indicating that *Bmal1* was knocked out, and furthermore, it was only being knocked out in endothelial cells (Figure 5C).

We also crossed a *VECad*-CreERT2 mouse to a *Rosa-loxstoplox-tdTomato* reporter mouse to visualize the precise location of Cre-recombination. Six weeks after tamoxifen treatment, we collected brains from both control and *VECad*-CreERT2; *Rosa-tdTomato* mice for immunohistochemistry. Through co-staining with endothelial cell marker CD31, we found that tomato colocalized with CD31, indicating that Cre recombination was specific to endothelial cells (Figure 5D).

#### *The endothelial-specific clock regulates ABC transporter function*

To address the endothelial-specific clock's role in ABC efflux transport, we performed a rhodamine permeability assay. We injected RH123 and collected both *Bmal1<sup>fl/fl</sup>* controls and *Bmal1<sup>fl/fl</sup>; VECad*-CreERT2 brains from each of the following time points: ZT 0, ZT 6, ZT 12, and ZT 18, where ZT 0 refers to lights on and ZT 12 refers to lights off. We performed this experiment to answer two questions: firstly, is there circadian oscillation in ABC transport function in control conditions, and secondly, does this circadian oscillation depend on the endothelial-specific clock? Control animals appeared to exhibit a cyclic functional permeability to RH123 with peak permeability at ZT 0 and trough permeability at ZT 12 (Figure 6A). However, sample sizes were small for several time points (ZT 0, n=7; ZT 6, n=3; ZT 12, n=4; ZT 18, n=2), and therefore statistics by one-way ANOVA were not significant. However, a pairwise comparison of RH123 permeability between ZT0 and ZT12 in control animals was statistically significant by a Student's t-test. This suggests that normal brain endothelial cells have differential permeability with respect to ABC transporters at these two time points. Specifically, there is greater permeability (less ABC

transport) at the end of the active period, and less permeability (more ABC transport) at the end of the rest period.

In *Bmal1* endothelial cell knockouts, there was no observable cyclical trend nor any statistically significant differences in RH123 permeability at the different time points. This suggests that control mice have a naturally oscillating rhythm in ABC transporter function in which there is low activity at the end of the active period and higher activity at the end of the rest period. But, when you knock out the clock in endothelial cells, that time-dependent permeability is abolished. In fact, ABC transporter function in knockouts seem to be regulated in the opposite direction for both time points, compared to controls.

#### *The endothelial-specific clock does not regulate circadian-driven behavior*

To address the question of whether manipulating the endothelial-specific clock will affect brain function and behavior, we first investigated canonical circadian-driven behaviors, namely feeding and drinking. We measured total food and water intake in *Bmal1<sup>fl/fl</sup>* controls and *Bmal1<sup>fl/fl</sup>; VECad-CreERT2* mice over a period of four days. By measuring amount of food/water consumed after every light and dark phase, we could observe whether circadian feeding and drinking behavior were disrupted in mice lacking *Bmal1* in endothelial cells. Both control mice and *Bmal1* endothelial knockout mice showed normal feeding and drinking behaviors, in which intake was higher during the dark phase and lower during the light phase (Figure 7A, B.). Overall, circadian regulation of feeding and drinking appeared to be unaffected by knocking out *Bmal1* in endothelial cells suggesting that the endothelial-specific circadian clock does not regulate circadian-related behaviors.

*The endothelial-specific clock does not regulate learning and memory behavior*

We next tested whether abolishing the clock in endothelial cells would affect learning and memory in the novel object recognition (NOR) test because *Bmal1* global knockouts have been shown to have deficits in long and short term memory (Kondratova, Dubrovsky, Antoch, & Kondratov, 2010). The NOR test evaluates the mouse's ability to distinguish a novel object from a familiar object. A mouse with normal learning and memory skills spends more time exploring a novel object compared to a familiar object, whereas a mouse with impaired learning and memory could spend equal or less time exploring the novel object. We first found that there was no statistically significant difference in the total amount of time spent exploring the objects in any of the trials between the controls and knockouts (Figure 8B), indicating the general exploratory behavior was not impaired in knockouts. In addition, there was no statistical difference in the discrimination index, the ability to discriminate the novel object from the old object (Figure 8C). This indicates that abolishing the clock in endothelial cells does not affect learning and memory behavior.

*The endothelial-specific clock does not regulate anxiety-related behavior, but does regulate depression-related behavior*

The final category of behavioral experiments we performed was for affect-related disorders, namely anxiety and depression. To evaluate anxiety-related behavior, we used the open field test. We found that for both controls and endothelial clock knockouts, the amount of time spent in the inner box was roughly equivalent, indicating no difference in anxiety-related behavior (Figure 9A).

We then investigated depression-related behavior using the tail suspension test, a commonly used behavioral paradigm for screening anti-depressant drugs. The test involves suspending the mouse by the tail and observing how much time it spends immobile, where immobility is a sign of learned helplessness. We found that endothelial-specific *Bmal1* knockouts had a significantly greater average immobility time compared to controls, indicative of depression-like behavior (Figure 9B). Because our model is affecting all endothelial cells of the body, the tail suspension results could potentially be attributed to a blood pressure or blood flow deficit in the entire vasculature, leading to greater lack of movement than in controls.

*Behavioral phenotypes observed are specific to the brain endothelial-clock*

Since the *VE-Cadherin-Cre* is specific to all endothelial cells of the body, is it possible that our behavioral results were due to knocking out the circadian clock in the peripheral vasculature as opposed to a specific role in the brain vasculature. Therefore, we created a second transgenic line, *Bmal1<sup>fl/fl</sup>; Slco1c1-CreERT2*, in which the Cre is expressed in brain endothelial cells and not peripheral endothelial cells. Once again, we performed circadian food and water intake measurements, novel object recognition test, open field test, and tail suspension test on these mice. For circadian food and water measurements, knockouts had normal oscillations in feeding and drinking, reflective of controls (Figure 10A). In the NOR test, knockouts had a slightly lower discrimination index, suggesting a potential learning and memory deficit, however the difference was not significant (Figure 10B). In the open field test, knockouts on average spent an equal amount of time in the center of the box (Figure 10C). In the tail suspension test, knockouts had a slightly higher immobility time, however the difference was not significant (Figure 10D). All behavioral experiments with this transgenic line had low sample sizes, but the preliminary data

seems to be reflective of the trends observed with the *VECad*-CreERT2 knockouts. In particular, the *Bmal1<sup>fl/fl</sup>*; *Slco1c1*-CreERT2 knockout mice exhibit slightly higher average immobility time in the tail suspension test compared to controls, which is consistent with the result we saw with pan-endothelial cell *Bmal1* knockouts.

## 2.4 Discussion

Through knocking out the master circadian regulator *Bmal1* in endothelial cells *in vivo*, we investigated the hypothesis that disrupting the clock in the brain vasculature would dysregulate circadian oscillations in ABC transporter-mediated BBB permeability, and modulate neuronal function, hence animal behavior. With respect to ABC transporter-mediated BBB permeability, we showed that control mice do have differential permeability at different times of day, implying that ABC transporter activity is subject to circadian oscillations. Additionally, knocking out the clock in endothelial cells caused this difference to be abolished. The data showing a potential circadian oscillation in ABC transporter activity could have profound implications for our understanding of their substrates. The data showing greater BBB permeability at the end of the active period in mice could advise when to administer neurological drugs that are substrates of P-gp, such that they cross the barrier with maximum efficiency in humans. It also could suggest that clearance of endogenous waste products, such as amyloid beta, is subject to a circadian oscillation specifically in endothelial cells.

With respect to animal behavior, we showed that whole-body endothelium deletion of *Bmal1* did not alter canonical circadian-driven behavior or learning and memory, however did display a depressive phenotype as assessed by the tail suspension test. We propose that the endothelial clock is regulating ABC efflux, and since ABC efflux is a major BBB property and

contributes to its overall function of regulating the brain's microenvironment, the disruption of the clock causes dysregulation of ABC efflux, which alters the microenvironment of the brain and leads to neuronal dysfunction and depression-related behavior. The ABC family have mostly been studied as drug transporters, but there is evidence that they also flux endogenous steroids. In fact, P-gp is an important regulator of aldosterone in the CNS. P-gp global knockout mice have higher aldosterone in the brain and have elevated anxiety-like behavior (Hindle et al. 2017). Together, this shows that disruptions in P-gp can affect neuronal circuitry sufficiently to cause complex behavioral phenotypes. Our results contribute to this claim by suggesting that the vascular clock is in control of P-gp activity, and so disruption of the clock leads to dysregulation of P-gp activity, and thus can cause a behavioral phenotype such as depression.

Interestingly, depression and other mood disorders have considerable evidence linking them to dysregulated circadian rhythms. Scientists theorize that mood disturbances result from phase shifts in the central pacemaker and its function in regulating body temperature, cortisol and melatonin levels, and REM sleep (Germain & Kupfer 2008). Other than phase shifts in SCN output, cerebral vascular disease has also been implicated as possible cause of depression. The "vascular depression" hypothesis proposes cerebrovascular defects have adverse effects on brain circuitry and contribute to the development of late-life depression in elderly people. Some of the current understanding of vascular depression is the development of white matter lesions due to impaired cerebral vasomotor reactivity and resulting ischemia (Taylor, Aizenstein, & Alexopoulos 2013). The underlying mechanisms of how this is occurring is not clear, but our finding that circadian disruption in endothelial cells leads to depression could be explained if endothelial Bmal1 regulates cerebral vascular tone, which is an avenue of this project that our lab will undertake in the future. We plan to use *in vivo* two-photon imaging of cerebral vessels to visualize

diameter changes over the course of the circadian day in both control and *Bmal1* endothelial cell knockouts. If the endothelial clock does indeed regulate vascular tone and its deletion leads to dysregulation of cerebral blood flow, it can provide a relationship between absence of the clock in the endothelium, vascular disease, and the depressive phenotype we saw in our studies.

As of now, our understanding of the *Bmal1*'s role in the cerebral vasculature using a *VE-Cadherin* driven CreERT2 is limited because there could be confounding effects from peripheral vascular defects. There has been considerable evidence showing that the clock is involved in mean arterial blood pressure and the development of hypertension in the periphery. Lack of blood flow to peripheral organs and muscles could account for greater immobility during the tail suspension test. Therefore, our lab plans to continue repeating all behavioral tests with *Bmal1<sup>fl/fl</sup>; Slco1c1-CreERT2* brain endothelial-specific knockouts. If we increase the sample size and observe the same result with the tail suspension test, we can be more confident that the brain vascular clock, as opposed to the entire vascular clock, plays a role in regulating animal behavior.

Lastly, an experiment that will be crucial to understanding the mechanisms of clock-controlled vascular properties is obtaining global RNA expression changes in endothelial cells over the course of 24 hours. This will reveal which genes in the cerebral vasculature naturally oscillate in a circadian manner. This will also reveal if these cerebral vascular genes are also under control of the vascular-specific clock if their circadian oscillation of expression is abolished by knocking out *Bmal1* in endothelial cells. However, since isolating endothelial cells by FACS for RNA extraction at multiple time points throughout the circadian day is not feasible, we plan to create RiboTagged endothelial-specific *Bmal1* conditional knockouts and littermate controls to enable time-sensitive purification of actively translated RNA (Sanz et al., 2009). RNA sequencing

of endothelial cell RNA every 6 hours will inform us of circadian-oscillating vascular genes, including *P-gp* and whether they are dependent on endothelial-specific Bmal1.

## GENERAL DISCUSSION

Overall, we have shown that glutamatergic neural activity directly regulates endothelial expression of many interesting genes, including those related to the BBB. This is interesting because previously, the BBB was considered a static structure that is either functioning in health or broken down in disease. However, our findings indicate that the cerebral vasculature is dynamically changing its molecular profile to regulate what can get into and out of the brain tissue based on amount of neural activity. Next, we found that the clock-controlled bZip transcription factors are also directly regulated by neural activity. This raises the question of whether neural activity actually entrains the endothelial-specific clock, similar to how light from the environment entrains the neurons of the SCN. We saw that control mice have higher permeability to RH123 at the end of their active period and less permeability at the end of their rest period, which is consistent with the same experiment performed in response to neural activity, in which we saw greater permeability in response to high activity and lower permeability in response low activity. Potentially, greater basal levels of neural activity during the active period and lower levels during the rest period signals to endothelial cells and drives the oscillation of clock machinery, which regulates ABC transport in a circadian manner, which regulates neurochemistry and behavior. Another important implication of brain endothelial clock-controlled ABC transport is for waste clearance from the brain during wake and sleep. Since we saw that permeability was greater both after a period of artificially increased neural activity (DREADDs) at the end of the circadian active period in mice (ZT 0), it opens up the possibility that for humans, high neural activity during the wake period regulates the brain endothelial-specific clock to turn on expression of *P-gp* at the end of the circadian day because built up metabolic waste products in the extracellular space are in need of clearance, which then occurs most efficiently when we sleep. Clearly, further work will

be required to unravel this story, but our research most strongly suggests the existence of brain endothelial clock regulated ABC efflux, which challenges current perspectives on the development of behavioral disorders, delivering therapeutics to the CNS, and the brain detoxification.

**Table 1. DAVID Pathway Analysis for 105 genes upregulated after glutamatergic activation and downregulated after glutamatergic activation**

<b>Cluster Number</b>	<b>Gene Functional Annotation</b>	<b>Enrichment Score</b>
1	Cell-cell Adherens Junction	4.95
2	Focal adhesion	4.11
3	RNA-binding	1.89
4	tRNA activity/Protein synthesis	1.24
5	WD40 repeat-containing domain	1.14
6	Ribonucleoprotein	0.99
7	Cell adhesion	0.97
8	Methylation	0.73
9	ATP/Nucleotide Binding	0.7
10	Transcriptional Regulation	0.68
11	Zinc Finger, LIM type	0.58
12	Mitochondrion	0.55
13	Nuclease Activity	0.54
14	Nervous System Development	0.44
15	Endoplasmic Reticulum	0.24

**Table 2. DAVID Pathway Analysis for 138 genes upregulated after glutamatergic silencing and downregulated after glutamatergic activation**

<b>Cluster Number</b>	<b>Gene Functional Annotation</b>	<b>Enrichment Score</b>
1	Transcriptional Regulation, DNA-binding	2.93
2	Chromo domain	2.71
3	Cytoskeleton	2.16
4	ABC transporters	1.95
5	Basic-leucine zipper domain, biological rhythms	1.88
6	Chromatin Regulation	1.59
7	C2 calcium-dependent membrane targeting	1.51
8	VEGF Signaling	1.38
9	ATP/Nucleotide Binding	1.38
10	Zinc Finger, PHD type	1.32
11	Phosphatidylinositol signaling	1.2
12	Pleckstrin Homology Domain	1.14
13	Proteoglycans in Cancer	1.13
14	EGF-like Domain	1.1
15	Synaptic Signaling	1.09

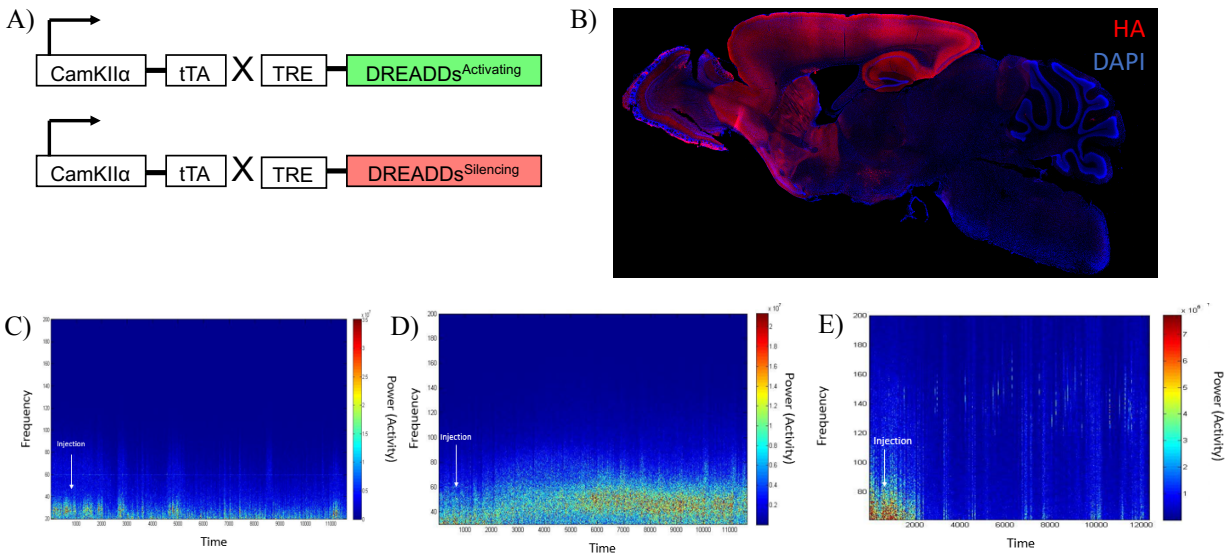


**Figure 1. Optimization of DREADDs in glutamatergic neurons.** A) CamKII $\alpha$ -tTA mice were crossed to Rosa-TRE-GqDREADDs and Rosa-TRE-GiDREADDs mice to express the activating and silencing DREADDs solely in glutamatergic neurons. B) Immunohistochemistry of a sagittal brain slice from a CamKII $\alpha$ -tTA; TRE-GqDREADDs mouse. HA in red and DAPI in blue. DREADDs under the CamKII $\alpha$  promoter are expressed in the cortex and hippocampus. C) Power density spectrum in littermate control mouse that did not express DREADDs indicated no observable change in gamma LFP power in response to a 1 mg/kg CNO injection. D) Power density spectrum in GqDREADDs mouse indicated increased gamma LFP power in response to 0.5 mg/kg CNO injection. E) Power density spectrum in GiDREADDs mouse indicated decreased gamma LFP power in response to 1 mg/kg CNO injection.

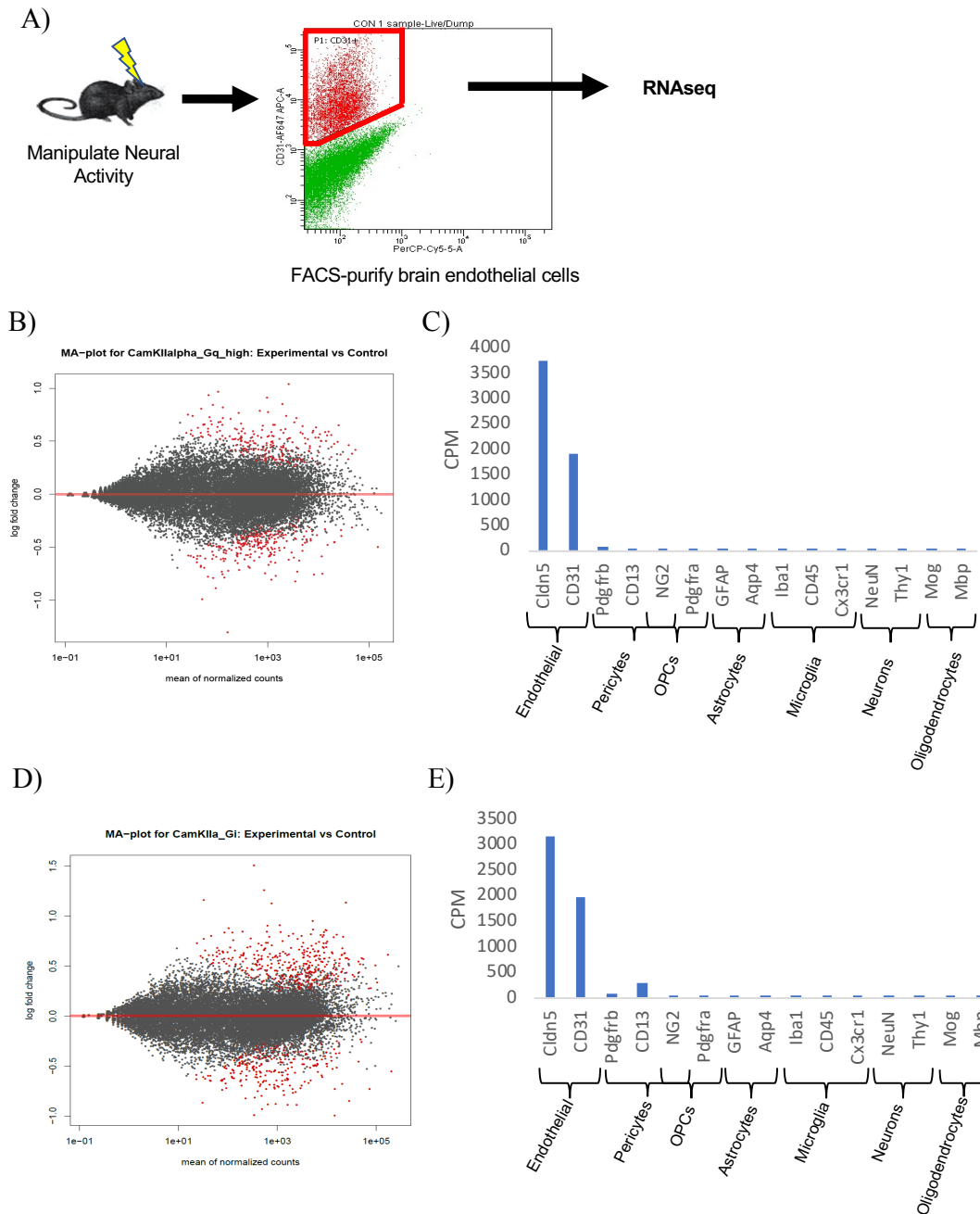


**Figure 2. Global gene expression of endothelial cells after manipulation of neural activity.** A) RNA sequencing workflow. Manipulation of neural activity was achieved by CNO injection to activating and silencing DREADDs mice along with littermate controls. 3 hours post injections, endothelial cells were isolated via FACS purification of CD31 positive cells, from which RNA was isolated for RNA sequencing. B and D) MA-plot of differential genes as a result of activating and silencing glutamatergic neurons, respectively. C and E) Analysis of endothelial cell sample purity by common cell markers, such as claudin 5 and CD31, in activating and silencing glutamatergic neurons.

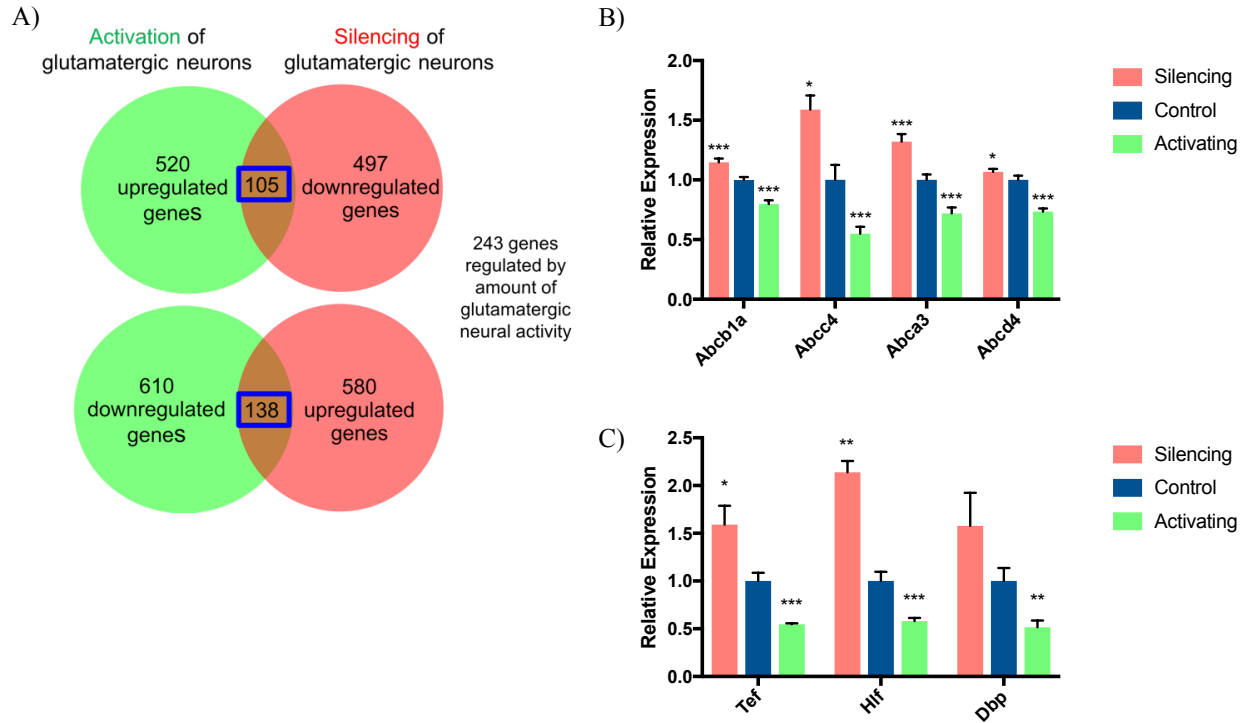


**Figure 3. Neural activity-dependent genes.** A) RNA sequencing revealed 105 genes that were both upregulated in GqDREADDs mice and downregulated in GiDREADDs mice, and also 138 genes that were both downregulated in GqDREADDs mice and upregulated in GiDREADDs mice. Altogether, we found 243 genes that changed in opposite directions after activation versus silencing of neural activity. B) ATP-binding cassette (ABC) transporters were of the genes that were upregulated after silencing and downregulated after activating. Data was plotted as mean expression relative to controls  $\pm$ SEM. C) Circadian clock-controlled PAR bZip transcription factors were of the genes that were upregulated after silencing and downregulated after activating. Data was plotted as mean expression relative to controls  $\pm$ SEM.

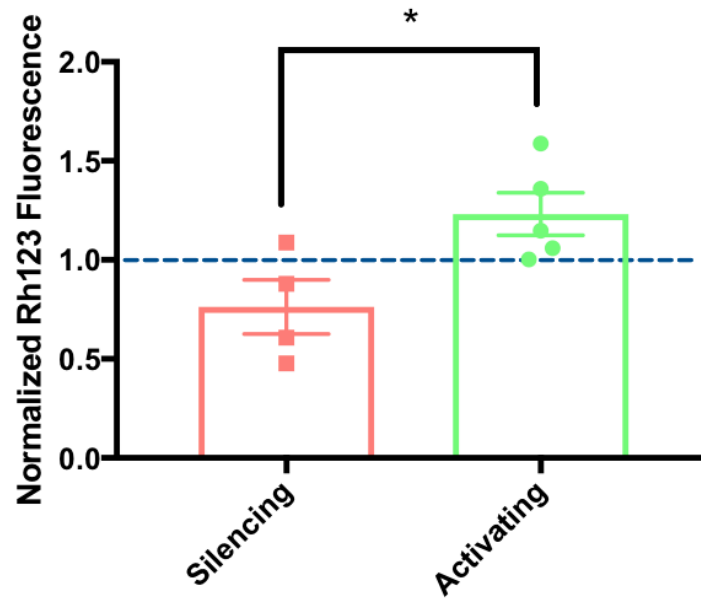


**Figure 4. ABC efflux transport function is regulated by neural activity.** BBB permeability to RH123 was assessed after three hours of silencing or activating glutamatergic neurons using DREADDs. RH123 fluorescence in the brain was normalized to RH123 fluorescence in the plasma. Data is plotted as mean normalized fluorescence relative to control (blue dotted line)  $\pm$ SEM. N=4 for silencing condition; N=5 for activating condition.  $p=0.0352$  (t-test)

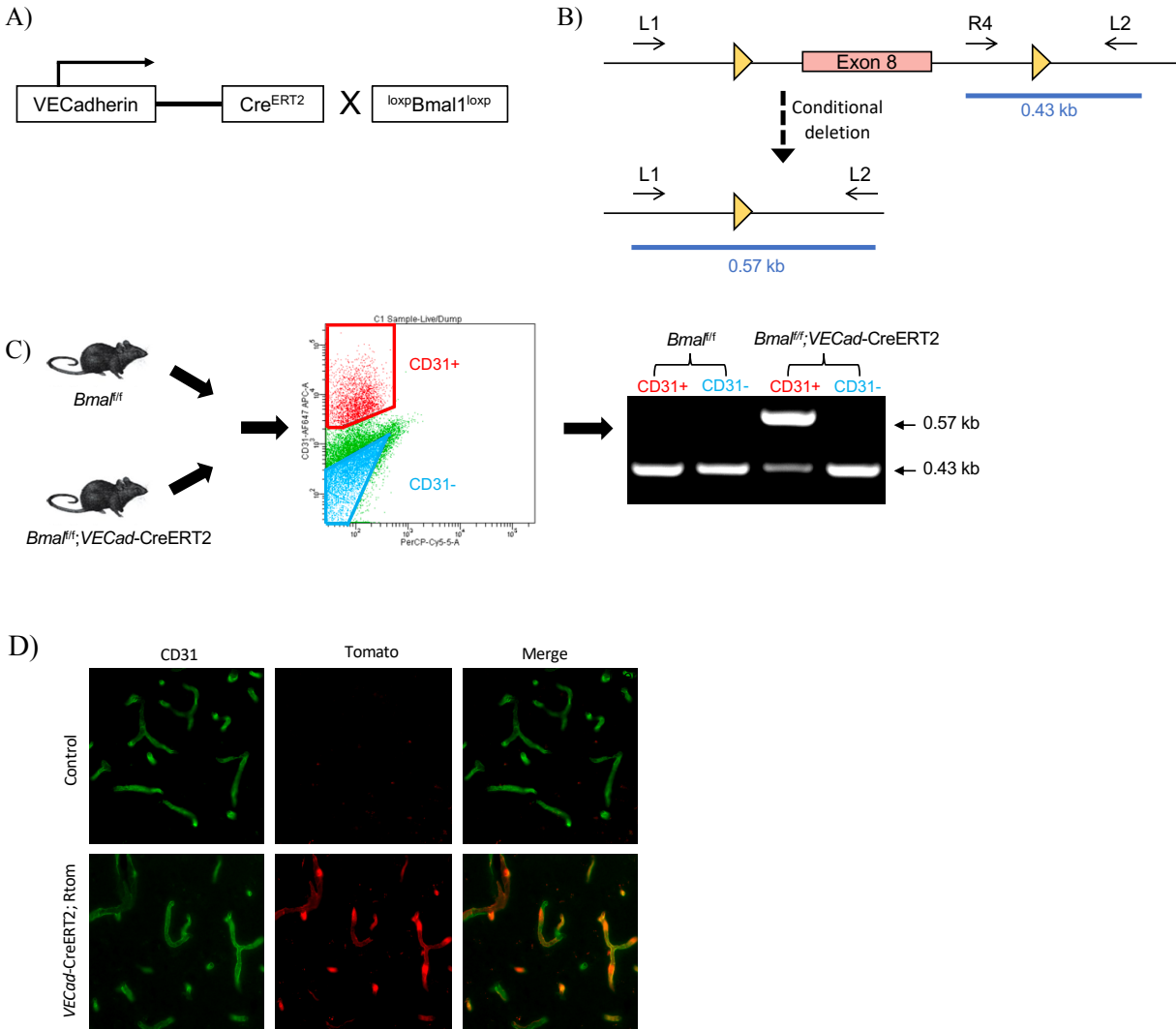


**Figure 5. Generation of endothelial cell *Bmal1* conditional knockout.** A) To knockout *Bmal1* specifically in all endothelial cells, a *VE-Cadherin-CreERT2* mouse was crossed to a mouse with a loxP-flanked basic helix-loop-helix (bHLH) domain of *Bmal1* to create *Bmal1<sup>f/f</sup>; VECad-CreERT2* mice and genetic controls (*Bmal1<sup>f/f</sup>*). B) Adapted from Storch et al 2007. The intact conditional allele with the bHLH region (exon 8) of the *Bmal1* gene flanked by two loxP sites (yellow triangles). After tamoxifen injection, Cre recombinase deletes exon 8, leaving a single loxP site. Black arrows indicate annealing positions of three PCR primers as described by Storch et al 2007. C) To confirm knockout, endothelial cells (CD31<sup>+</sup>) and non-endothelial cells (CD31<sup>-</sup>) were purified from control and endothelial *Bmal1* knockouts by FACS. DNA was isolated and genotyping performed using PCR primers L1, L2, and R4. Only endothelial cells from the knockout revealed the conditionally deleted allele. D) *Bmal1<sup>f/f</sup>; VECad-CreERT2* mice were crossed to a *Rosa-loxstoplox-tdTomato* reporter mouse. CD31 in green, tomato in red. 80x magnification.

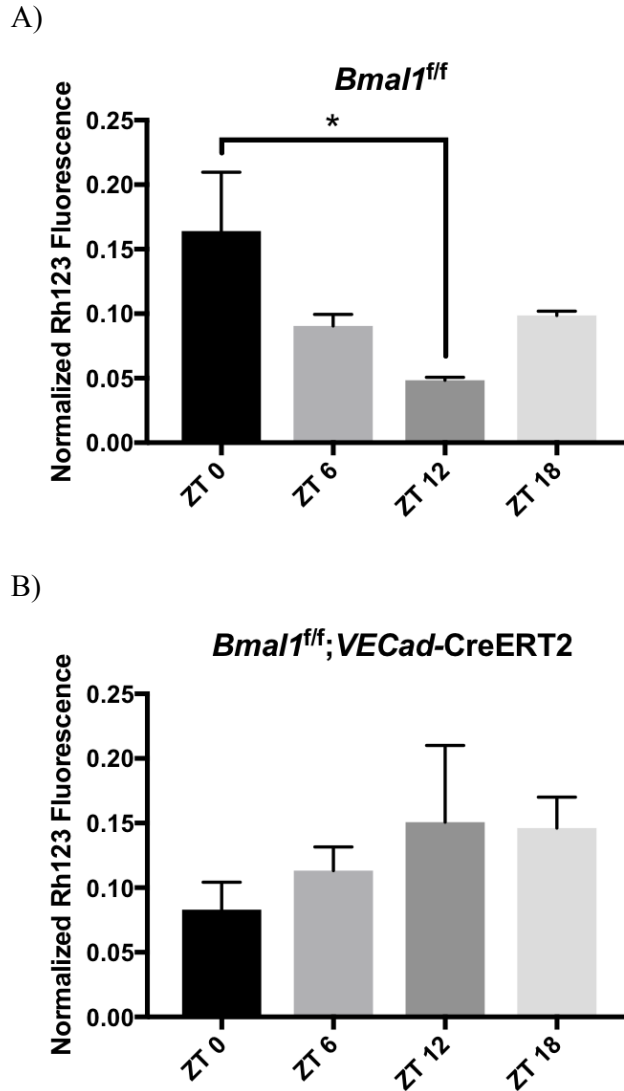


**Figure 6. The endothelial-specific clock regulates time-of-day dependent ABC efflux.** A) Rhodamine123 permeability assay for control mice at four time points. RH123 fluorescence in the brain was normalized to RH123 fluorescence in the plasma. Data is plotted as mean normalized fluorescence  $\pm$ SEM. ZT 0, N=7; ZT 6, N=3; ZT 12, N=4; ZT 18, N=2.  $p=0.0442$  (t-test). B) Rhodamine123 permeability assay for endothelial *Bmal1* knockout mice at four time points. RH123 fluorescence in the brain was normalized to RH123 fluorescence in the plasma. Data is plotted as mean normalized fluorescence  $\pm$ SEM. ZT 0, N=5; ZT 6, N=3; ZT 12, N=5; ZT 18, N=3).

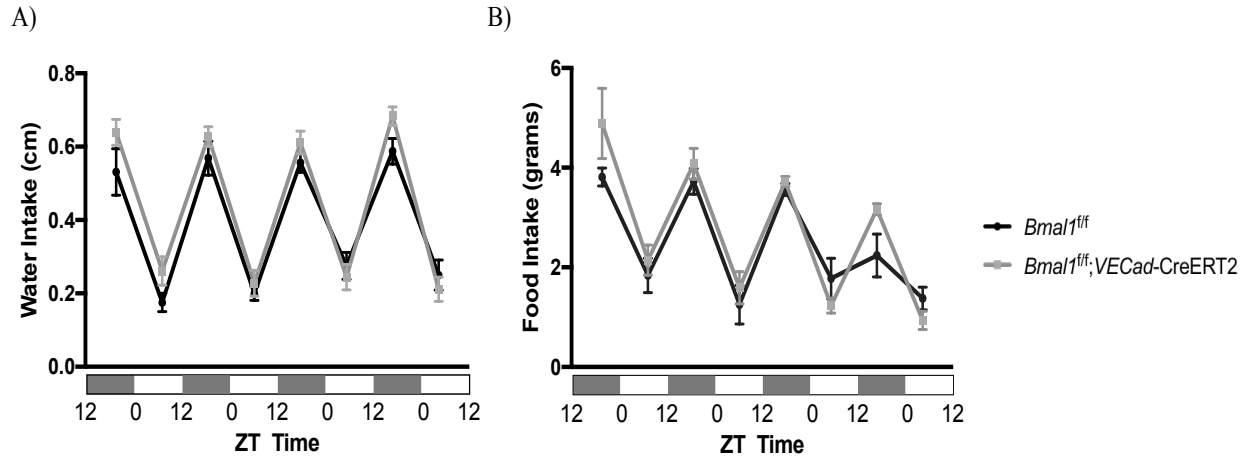


**Figure 7. The endothelial-specific clock does not regulate circadian-driven feeding and drinking behaviors.** Mice were held on a standard light (ZT 0-12)/ dark (ZT12-24) cycle and provided normal chow and water *ad libitum*. N=3 for *Bmal1<sup>fl/fl</sup>* controls and N=4 for *Bmal1<sup>fl/fl</sup>;VECad-CreERT2* knockouts. A) The mean water intake was measured by displacement of water in a cylindrical tube in cm  $\pm$ SEM of each group during each light and dark phase over four days. B) Food intake was measured by weight in grams  $\pm$ SEM of each group during each light and dark phase over four days.

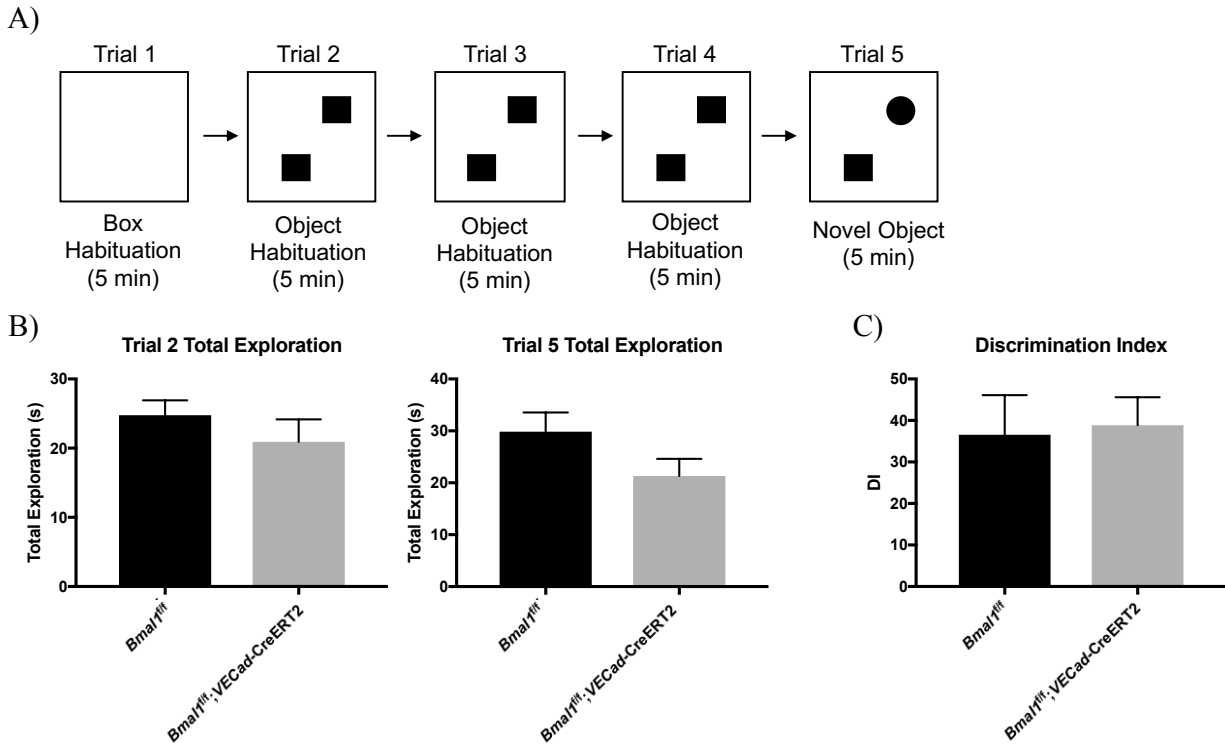


**Figure 8. Endothelial-specific *Bmal1* knockout does not affect learning and memory.** A) The novel object recognition test. Mice were habituated to the testing box for 5 minutes, then habituated to two identical objects for 5 minutes, x3 trials. One object was replaced by a novel object. Mice were scored on how much time they spent exploring each object. B) Total time spent exploring any object in trials 2 and 5. C) Discrimination index was calculated as time spent exploring novel object subtracted by time spent exploring familiar object, divided by total exploration time in trial 5. Data is plotted as mean  $\pm$  SEM. N=14 for each condition.

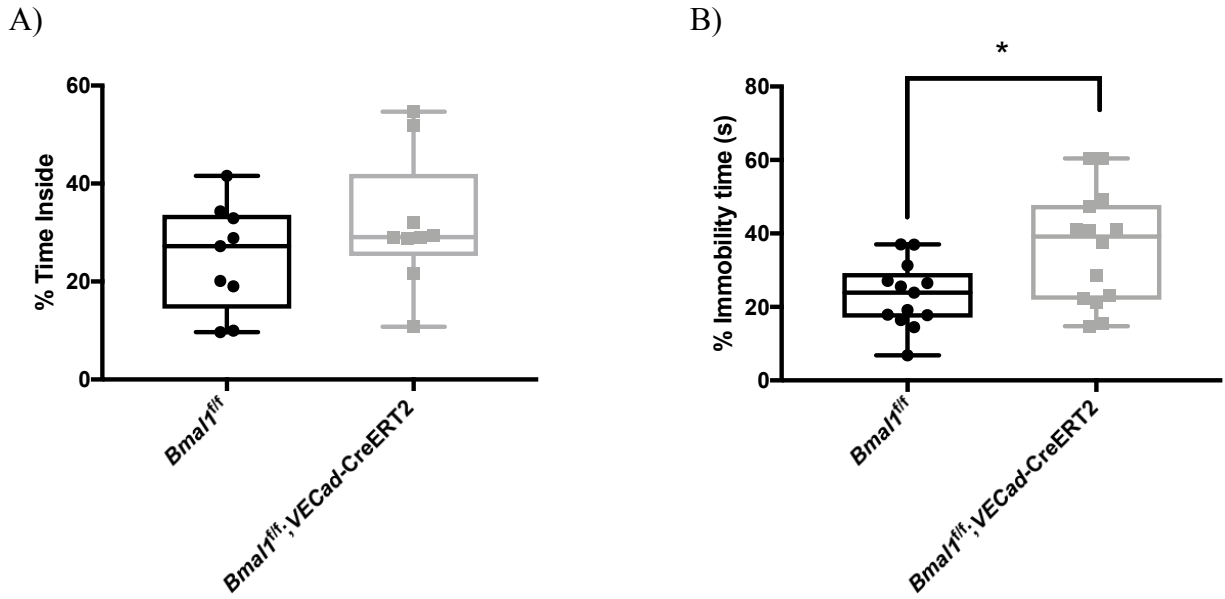


**Figure 9. Endothelial-specific *Bmal1* knockout displays depression-related behavior, but not anxiety-related behavior.** A) The open field test. Mice were placed in the testing arena and scored for amount of time spent inside an inner drawn square, as opposed to around the perimeter of the testing arena. Data is plotted as mean  $\pm$ SEM. N=9 for both conditions. B) The tail suspension test. Mice were suspended above the ground by the tail and scored for the amount of time spent hanging immobile, as opposed to displaying “escape”-like behavior. Endothelial *Bmal1* knockouts had a significantly greater immobility time compared to controls. Data is plotted as mean  $\pm$ SEM. N=13 for  $Bmal1^{fl/fl}$ , N=14 for  $Bmal1^{fl/fl}; VECad-CreERT2$ . p=0.0140 (t-test).

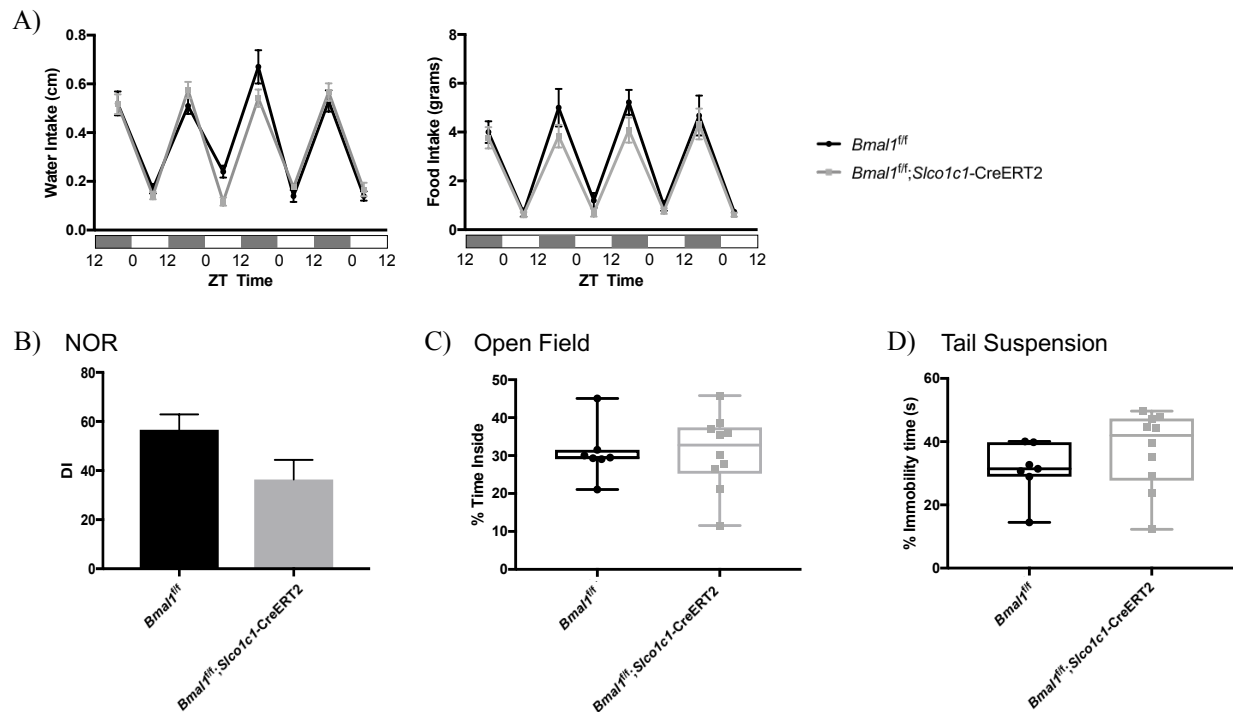


**Figure 10. Brain-endothelial specific *Bmal1* knockout behavioral trends.** All behavioral tests were performed on *Bmal1<sup>fl/fl</sup>* control and *Bmal1<sup>fl/fl</sup>; Slco1c1-CreERT2* knockout mice to test whether previously observed effects were specific to brain endothelial cells. All data are plotted as mean  $\pm$  SEM. A) Circadian water and food intake for control and brain endothelial knockouts over four days. N=5 for control, N=6 for brain endothelial knockout. B) Novel object recognition test. N=6 for control, N=7 for brain endothelial knockout. C) Open field test. N=7 for control, N=10 for brain endothelial knockout. D) Tail suspension test. N=7 for control, N=10 for brain endothelial knockout. Knockouts show slightly higher average immobility time compared to controls.

## REFERENCES

- Abbott, N. J., Rönnbäck, L., & Hansson, E. (2006). Astrocyte-endothelial interactions at the blood-brain barrier. *Nature Reviews Neuroscience*, 7(1), 41–53.
- Alexander, G. M., Rogan, S. C., Abbas, A. I., Armbruster, B. N., Pei, Y., Allen, J. A., Nonneman, R. J., Hartmann, J., Moy, S. S., Nicoletis, M. A., McNamara, J. O., Roth, B. L. (2009). Remote control of neuronal activity in transgenic mice expressing evolved G protein-coupled receptors. *Neuron*, 63(1), 27–39.
- Alvarez, J. I., Cayrol, R., & Prat, A. (2011). Disruption of central nervous system barriers in multiple sclerosis. *Biochimica et Biophysica Acta - Molecular Basis of Disease*, 1812(2), 252–264.
- Anderson, J. M., & Van Itallie, C. M. (2009). Physiology and function of the tight junction. *Cold Spring Harbor Perspectives in Biology*, 1(2), 2584–2585.
- Anea, C. B., Cheng, B., Sharma, S., Kumar, S., Caldwell, R. W., Yao, L., Ali, M. I., Merloiu, A. M., Stepp, D. W., Black, S. M., Fulton, D. J., Rudic, R. D. (2012). Increased superoxide and endothelial NO synthase uncoupling in blood vessels of Bmal1-knockout mice. *Circulation Research*, 111(9), 1157–1165.
- Banes, A. J., Link, G. W., Beckman, W. C., Camps, J. L., & Powers, S. K. (1986). High-performance liquid chromatographic quantitation of rhodamines 123 and 110 from tissues and cultured cells. *Journal of Chromatography A* (Vol. 356).
- Bevilacqua, M. P. (1993). Endothelial-leukocyte adhesion molecules. *Annu. Rev. Immunol.* 11, 767-804
- Cordon-Cardo, C., O'Brien, J. P., Casals, D., Rittman-Grauer, L., Biedler, J. L., Melamed, M. R., & Bertino, J. R. (1989). Multidrug-resistance gene (P-glycoprotein) is expressed by endothelial cells at blood-brain barrier sites. *Proceedings of the National Academy of Sciences* (Vol. 86).
- Curtis, A. M., Cheng, Y., Kapoor, S., Reilly, D., Price, T. S., & Fitzgerald, G. A. (2007). Circadian variation of blood pressure and the vascular response to asynchronous stress. *Proceedings of the National Academy of Sciences of the United States of America*, 104(9), 3450–3455.
- Durgan, D. J., Crossland, R. F., & Bryan, R. M. (2017). The rat cerebral vasculature exhibits time-of-day-dependent oscillations in circadian clock genes and vascular function that are attenuated following obstructive sleep apnea. *Journal of Cerebral Blood Flow and Metabolism*, 37(8), 2806–2819.
- Engelhardt, B. (2008). Immune cell entry into the central nervous system: Involvement of adhesion molecules and chemokines. *Journal of the Neurological Sciences*. 274, 23-26.

- Erickson, M. A., & Banks, W. A. (2013). Blood-brain barrier dysfunction as a cause and consequence of Alzheimer's disease. *Journal of Cerebral Blood Flow and Metabolism*, 33(10), 1500–1513.
- Faucheux, B. A., Bonnet, A. M., Agid, Y., & Hirsch, E. C. (1999). Blood vessels change in the mesencephalon of patients with Parkinson's disease. *Lancet*, 353(9157), 981–982.
- Fergus, A., & Lee, K. S. (1997). Regulation of cerebral microvessels by glutamatergic mechanisms. *Brain Research* (Vol. 754).
- Gachon, F., Fonjallaz, P., Damiola, F., Gos, P., Kodama, T., Zakany, J., Duboule, D., Petit, B., Tafti, M., Schibler, U. (2004). The loss of circadian PAR bZip transcription factors results in epilepsy. *Genes & Development*, 18, 1397-1412.
- Gachon, F., Olela, F. F., Schaad, O., Descombes, P., & Schibler, U. (2006). The circadian PAR-domain basic leucine zipper transcription factors DBP, TEF, and HLF modulate basal and inducible xenobiotic detoxification. *Cell Metabolism*, 4(1), 25–36.
- Germain, A., & Kupfer, D. J. (2008). Circadian rhythm disturbances in depression. *Human Psychopharmacology*, 23(7), 571–585.
- Henninger, D. D., Panés, J., Eppihimer, M., Russell, J., Gerritsen, M., Anderson, D. C., & Granger, D. N. (1997). Cytokine-induced VCAM-1 and ICAM-1 expression in different organs of the mouse. *Journal of Immunology (Baltimore, Md. : 1950)*, 158(4), 1825–1832.
- Hindle, S. J., Munji, R. N., Dolgih, E., Gaskins, G., Orng, S., Ishimoto, H., Soung, A., DeSalvo, M., Kitamoto, T., Keiser, M. J., Jacobson, M. P., Daneman, R., Bainton, R. J. (2017). Evolutionarily Conserved Roles for Blood-Brain Barrier Xenobiotic Transporters in Endogenous Steroid Partitioning and Behavior. *Cell Reports*, 21(5), 1304–1316.
- Hnasko, R., McFarland, M., & Ben-Jonathan, N. (2002). Distribution and characterization of plasmalemma vesicle protein-1 in rat endocrine glands. *Journal of Endocrinology* (Vol. 175).
- Howarth, C. (2014). The contribution of astrocytes to the regulation of cerebral blood flow. *Frontiers in Neuroscience*, 8(103).
- Igarashi, Y., Utsumi, H., Chiba, H., Yamada-Sasamori, Y., Tobioka, H., Kamimura, Y., Furuuchi, K., Kokai, Y., Nakagawa, T., Mori, M., Sawada, N. (1999). Glial cell line-derived neurotrophic factor induces barrier function of endothelial cells forming the blood-brain barrier. *Biochemical and Biophysical Research Communications* (Vol. 261).
- Karnovsky, M. J. (1968). The ultrastructural basis of transcapillary exchanges. *The Journal of General Physiology* (Vol. 52).

- Kondratova, A. A., Dubrovsky, Y. V., Antoch, M. P., & Kondratov, R. V. (2010). Circadian clock proteins control adaptation to novel environment and memory formation. *Aging*, *2*(5), 285–297.
- Lamas, M., González-Mariscal, L., & Gutiérrez, R. (2002). Presence of claudins mRNA in the brain. Selective modulation of expression by kindling epilepsy. *Brain Research. Molecular Brain Research*, *104*(2), 250–254.
- Longden, T. A., Dabertrand, F., Koide, M., Gonzales, A. L., Tykocki, N. R., Brayden, J. E., Hill-Eubanks, D., Nelson, M. T. (2017). Capillary K<sup>+</sup>-sensing initiates retrograde hyperpolarization to increase local cerebral blood flow. *Nature Neuroscience*, *20*(5), 717–726.
- Musiek, E. S., Lim, M. M., Yang, G., Bauer, A. Q., Qi, L., Lee, Y., Roh, J. H., Ortiz-Gonzalez, X., Dearborn, J. T., Culver, J. P., Herzog, E. D., Hogenesch, J. B., Wozniak, D. F., Dikranian, K., Giasson, B. I., Weaver, D. R., Holtzman, D. M., Fitzgerald, G. A. (2013). Circadian clock proteins regulate neuronal redox homeostasis and neurodegeneration. *The Journal of Clinical Investigation*, *123*(12).
- Nakazato, R., Kawabe, K., Yamada, D., Ikeno, S., Mieda, M., Shimba, S., Hinoi, E., Yoneda, Y., Takarada, T. (2017). Disruption of *Bmal1* impairs blood—brain barrier integrity via pericyte dysfunction. *The Journal of Neuroscience*, *37*(42), 3639–16.
- Newman, E. A. (2013). Functional hyperemia and mechanisms of neurovascular coupling in the retinal vasculature. *Journal of Cerebral Blood Flow and Metabolism*, *33*(11), 1685–1695.
- Reppert, S. M., & Weaver, D. R. (2001). Molecular Analysis of Mammalian Circadian Rhythms. *Annual Review of Physiology*, *63*(1), 647–676.
- Reppert, S. M., & Weaver, D. R. (2002). Coordination of circadian timing in mammals. *Nature*, *418*(6901), 935–941.
- Rgen, J., Ripperger, A., Shearman, L. P., Reppert, S. M., & Schibler, U. (2000). CLOCK, an essential pacemaker component, controls expression of the circadian transcription factor DBP. *Genes & Development*, *14*, 697-689.
- Richards, J., Diaz, A. N., & Gumz, M. L. (2014). Clock genes in hypertension: Novel insights from rodent models. *Blood Pressure Monitoring*, *19*(5), 249–254.
- Richards, J., & Gumz, M. L. (2012). Advances in understanding the peripheral circadian clocks. *The FASEB Journal*, *26*(9), 3602–3613.
- Ripperger, J. a, & Schibler, U. (2001). Circadian regulation of gene expression in animals. *Curr. Op. Cell Biol.*, *13*, 357–362.
- Sandoo, A., van Zanten, J. J. C. S. V., Metsios, G. S., Carroll, D., & Kitas, G. D. (2010). The

- endothelium and its role in regulating vascular tone. *The Open Cardiovascular Medicine Journal*, 4, 302–312.
- Sanz, E., Yang, L., Su, T., Morris, D. R., McKnight, G. S., & Amieux, P. S. (2009). *Cell-type-specific isolation of ribosome-associated mRNA from complex tissues. Proceedings of the National Academy of Sciences* (Vol. 106).
- Simpson, I. A., Carruthers, A., & Vannucci, S. J. (2007). Supply and demand in cerebral energy metabolism: the role of nutrient transporters. *Journal of Cerebral Blood Flow & Metabolism*, 27, 1766–1791.
- Stewart, P. A., & Wiley, M. J. (1981). Developing nervous tissue induces formation of blood-brain barrier characteristics in invading endothelial cells: A study using quail-chick transplantation chimeras. *Developmental Biology* (Vol. 84).
- Storch, K. F., Paz, C., Signorovitch, J., Raviola, E., Pawlyk, B., Li, T., & Weitz, C. J. J. (2007). Intrinsic Circadian Clock of the Mammalian Retina: Importance for Retinal Processing of Visual Information. *Cell*, 130(4), 730–741.
- Taylor, W. D., Aizenstein, H. J., & Alexopoulos, G. S. (2013). The vascular depression hypothesis: mechanisms linking vascular disease with depression. *Molecular Psychiatry*, 18, 963–974.
- Welsh, D. K., Logothetis, D. E., Meister, M., & Reppert, S. M. (1995). Individual neurons dissociated from rat suprachiasmatic nucleus express independently phased circadian firing rhythms. *Neuron*, 14(4), 697–706.
- Zhang, S. L., Yue, Z., Arnold, D. M., Artiushin, G., & Sehgal, A. (2018). A Circadian Clock in the Blood-Brain Barrier Regulates Xenobiotic Efflux. *Cell*, 173(1), 130–139.e10.
- Zlokovic, B. V. (2008). The Blood-Brain Barrier in Health and Chronic Neurodegenerative Disorders. *Neuron*, 57(2), 178–201.